Catalysis Letters
https://doi.org/10.1007/s10562-021-03721-6

Solvent-Driven Selectivity on the One-Step Catalytic Synthesis of Manoyl Oxide Based on a Novel and Sustainable "Zeolite Catalyst–Solvent" System

Dimitra Makarouni[1,2] · **Christos Kordulis**[1,3,4] · **Vassilis Dourtoglou**[2,5]

Received: 10 February 2021 / Accepted: 28 June 2021

Abstract

Application of a novel "zeolite catalyst–solvent" system for the sustainable one-step synthesis of the terpenoid manoyl oxide, the potential precursor of forskolin and ambrox. Manoyl oxide high-yield and large-scale production over a zeolite catalyst has been infeasible so far, while this system results in 90% yields at 135 °C and atmospheric pressure. Substrate-controlled methodology is used to achieve selectivity. Solvent-driven catalysis is shown, as the activation energy barrier decreases in the presence of appropriate solvents, being 62.7 and 93.46 kJmol^{-1} for a glyme-type solvent and dodecane, respectively. Finally, catalyst acidity is key parameter for the process.

Graphic Abstract

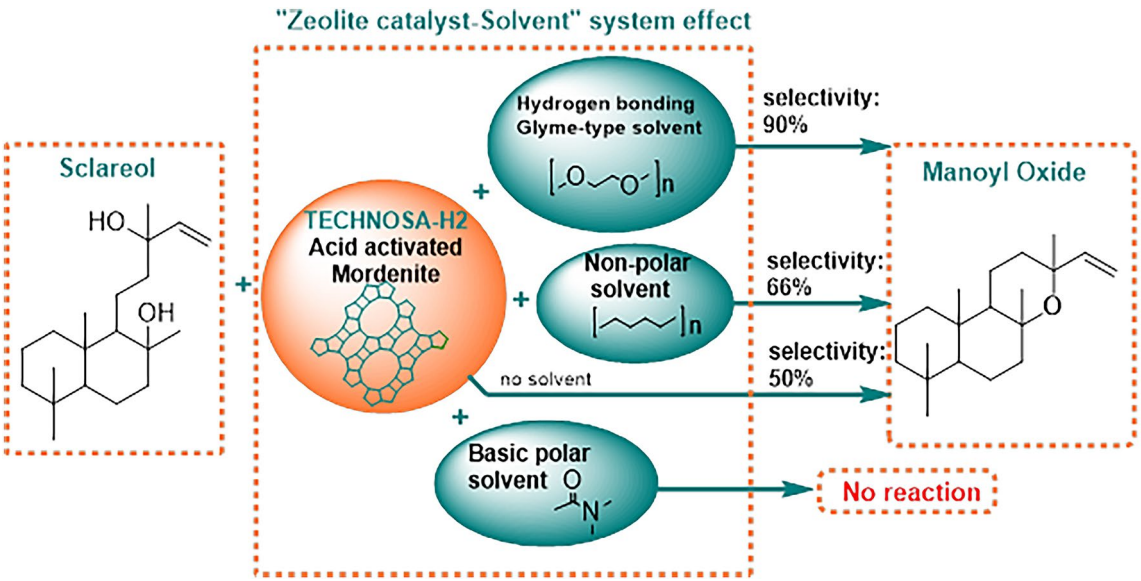

Keywords Manoyl oxide · Solvent effects · Zeolites · Cyclization · Heterogeneous catalysis · Terpenoids · Green chemistry · Acid catalysis · Dehydration · Activation energy

✉ Vassilis Dourtoglou
vdourt@uniwa.gr

Extended author information available on the last page of the article

Published online: 13 July 2021

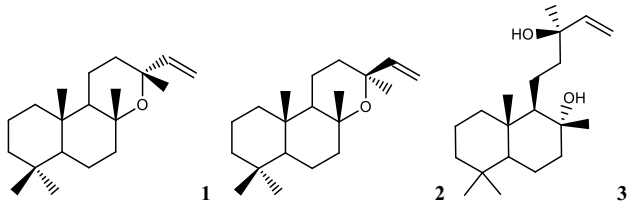

Scheme 1 Structures of manoyl oxide epimers **1, 2** and sclareol **3**

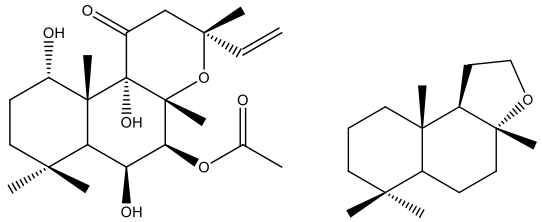

Scheme 2 Structure of forskolin (left) and ambrox (right)

1 Introduction

Cyclic ethers are fundamental heterocycles of bioactive compounds, natural products, etc. [1–3]. Therefore, the use of cyclodehydration reactions is of significant importance in the chemical industry.

The cyclic ether manoyl oxide (MO) is a compound that belongs to labdane diterpenes and is known to exhibit a number of important properties. MO is a compound of general formula $C_{20}H_{34}O$ and a mixture of two C13 epimers; 13R-MO (compound **1** in Scheme 1) and 13S-MO (compound **2** in Scheme 1) [4–6].

Both C13 MO epimers are valuable compounds as they have been proven to be an antibacterial agents against *Staphylococcus aureus*, *Pseudomonas aeruginosae* and *Klebsiella pneumonia* [7], as well as to have antimicrobial activity against *Borrelia burgdorferi* [8] and against Gram-positive bacteria (*B. cereus, Str.faecalis, St. aureus, St. epidermidis*, and *B. subtilis*) [9].

Furthermore, 13R-MO has been reported as a potential precursor of two valuable compounds forskolin [6, 10, 11] and ambrox [12–14] (Scheme 2). These two compounds have received much attention for their broad range of applications [13–21]. In particular, the limited availability of pure forskolin is currently hindering its full utilization; therefore, a new and sustainable strategy is needed for forskolin production. Recently, the entire biosynthetic pathway leading to forskolin was elucidated. A key process of this pathway include the biosynthesis of 13R-MO from GGPP (geranylgeranyl diphosphate), as 13R-MO consists the diterpene backbone of forskolin [10, 22, 23]. Then 13R-MO is further bioconverted to forskolin [24, 25]. Recent work has improved the efficiency towards forskolin biosynthesis in yeast from 13R-MO [25]. However, the optimization of the first step of the process i.e. the synthesis of 13R-MO, still remains a challenge. Maybe a solution to this challenge would be to replace the total biosynthetic pathway for the synthesis of Forskolin, by a process that combines a chemical pathway for the synthesis of 13R-MO, followed by a biosynthetic one for the synthesis of Forskolin from 13R-MO.

A number of synthetic procedures for the production of MO have been reported. Most of them start from sclareol (compound **3** in Scheme 1), which is a diterpene found in Clary Sage (Salvia sclarea). However, the already developed processes lead to relatively low yields of MO or comprise multistep procedures [26, 27].

Prior art includes also patents on the production of MO or cycloether derivatives by the cyclodehydration of diols, such as US10208326B2 [28] and US9469622B2 [29], respectively. Nevertheless, in US10208326B2 [28] a biosynthetic method of 13R-MO is proposed where long preparation/processing times are involved, while US9469622B2 [29] has the limitation that either high temperature water (HTW) conditions should be followed, or at least one of the hydroxyl groups of the diol must be non-tertiary and therefore production of MO from sclareol is not possible according to the means of this patent, or long reaction times are required (30 h). In addition, in the process described by Alvarez-Manzaneda EJ, Chaboun R., Alvarez E. et al. cerium (IV) ammonium nitrate (CAN) is utilized for the synthesis of MO from sclareol, but reaction times up to 10 h and stoichiometric amounts of CAN are required [30]. Previous work also includes processes were 90% yield in MO is achieved, by using trifluoroacetic acid in dioxane solution [31]. The drawbacks of such process include the employment of corrosive reagents as trifluoroacetic acid, while dioxane is classified from ECHA (Europpean Chemicals Agency) as a substance suspected of causing cancer. Finally, recent research includes the production of a 13R-MO yeast cell factory from glucose, but such process requires metabolic engineering strategies and long fermentation times [32].

Recently in EP3409663A1 [33] we have presented a new "zeolite catalyst–solvent", which can transform the diol sclareol to the cyclic ether MO with excellent selectivity in a one-step process over a mordenite catalyst. This novel system lead to yields in MO higher than 85%.

Solid catalysts have the advantage of being easily separated from the reaction mixture. However, a challenge of solid catalysts is that sometimes their various active sites can accelerate side reactions leading to undesired by–products. One solution to this problem could be the use of a solvent-controlled methodology to obtain high selectivity. In particular, fine chemicals synthesis over heterogeneous

catalysts sometimes involves the use of solvents that can strongly influence the catalytic performance [34–37]. In order to find the most appropriate solvent, it is essential to examine extensively the relationship between the chemical nature of the solvents and their interaction with the catalyst and the substrate [38–40].

Herein, we provide a step forward towards EP3409663A1 [33] and propose that solvent nature is a key parameter for the process, as a substrate-controlled methodology is used to achieve selectivity.

In particular, a zeolite acid catalyst (TECHNOSA–H2) prepared by acid activation of natural mordenite from volcanic soils [41, 42] was combined with various solvents. The efficiency of the corresponding "zeolite catalyst–solvent" systems for the dehydration of sclareol to MO was thoroughly investigated. The solvents examined were of different boiling points and polarities, in order to not only identify the most appropriate solvent from a yield standpoint, but also understand the mechanistics of the aforementioned system.

Considering the sustainability of the process, reaction conditions were optimized to develop a cost-effective and low energy-consuming method for providing high yield of MO by an easily applicable in industrial scale one-step process. In addition, in frame of utilizing renewable raw materials for chemical synthesis, the employment of acid treated natural mordenite as catalyst offers a low-cost and renewable catalyst alternative for the studied reaction.

Finally, the effects of catalyst's surface area and acidity were also inspected by testing two additional catalyst samples suitably modified to have different surface areas and acidities.

2 Experimental

2.1 Materials

Sclareol extracted by Salvea Sclarea and the natural mordenite catalysts (TECHNOSA-H2, TECHNOSA-H2C and TECHNOSA-A2) were supplied by VIORYL S.A. The glycol ethers (diglyme, triglyme and tetraglyme) were provided by BASF. The solvents (1,4-dioxane, dimethylformamide and tetrahydrofuran) were supplied by Fisher Scientific, dodecane by Sigma-Aldrich and hexane was purchased from Carlo Erba.

2.2 Catalyst Preparation and Characterization

Natural mordenite was stirred with distilled water for 2 h in a solid mass to liquid volume ratio 1 g/3 mL and the undesirable materials were removed by filtering. The slurry was dried for 2 h at 90 °C and then it was grinded to become fine-grained. This material was treated with 2 M acidic solutions of HCl, and CH_3COOH (all purchased by Fisher scientific) at 70 °C for 4 h and mass solid to solution volume 1 g/20 mL. Full details on the acid activation process have been reported previously [41, 42]. The symbols TECHNOSA-H2, and TECHNOSA-A2 stand, respectively, for the catalysts resulted by activation of natural mordenite with 2 M hydrochloric and acetic acid aqueous solutions. TECHNOSA-H2C catalyst was prepared by air-calcination of TECHNOSA-H2 catalyst at 500 °C for 2 h. Full characterization of TECHNOSA-H2, TECHNOSA-A2 and TECHNOSA-H2C with N_2-physisorption, XRD, ATR-FTIR, SEM–EDS, TEM, Microelectrophoresis and Equilibrium pH measurements have been reported elsewhere [42, 43]

2.3 Catalytic Conversion of Sclareol

One gram sclareol (Mw = 308.5 g/mol), 3 g of the selected glyme solvent and catalyst (0.9% mass ratio of sclareol) were combined in a round bottom flask equipped with a condenser. The flask was added in a preheated oil bath at the determined temperature and the mixture was stirred vigorously at a predetermined time. At the end of the reaction, the mixture was cooled at 25 °C, hexane was added, and the mixture was filtered to remove the catalyst. The filtrate was double washed with water and dried over anhydrous sodium sulfate. Finally, hexane removal was performed by condensation. The isolated product gave 0.84 g MO (MW = 290.5 g/mol). In other tests, the reaction was also performed in a solvent-free system. The same procedure as above was followed except from the initial addition of the solvent.

2.4 Analysis

The reaction mixture was analyzed by gas chromatography-mass spectrometry (Shimadzu GCMS-QP2010 Ultra equipped with capillary column: 20 m × 0.18 mm × 0.18 μm (using He as carrier gas), in addition to gas chromatography (AGILENT Technologies 6890 N with FID detector, using a Varian capillary column CP Sil 5 CB 25 m × 0.25 mm × 0.25 μm and He as the carrier gas). The identification of all compounds was performed using the mass spectra libraries of VIORYL S.A. and where necessary confirmation with analytical standards. All activity evaluation experiments were repeated at least three times and the standard error was found lower than ± 3%.

3 Results and Discussion

3.1 Catalytic Activity and Reaction Mechanism

Preliminary experiments, which have been performed without catalyst, have shown that sclareol is not transformed into

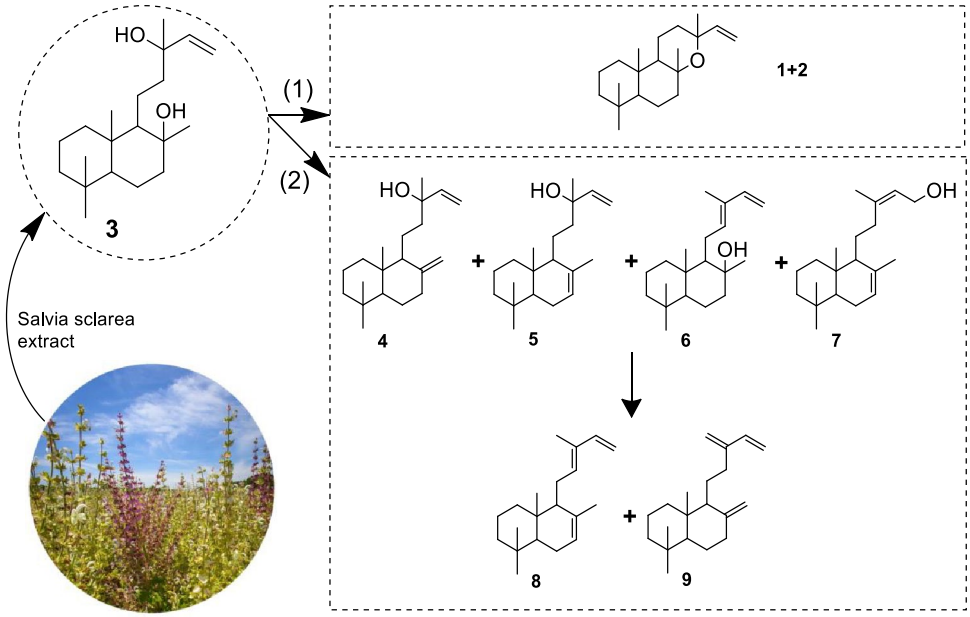

Scheme 3 Mechanistic proposal for the catalytic dehydration of sclareol over TECHNOSA-H2 catalyst. Pathway (1): cyclization of sclareol **3** to produce manoyl oxide **1** + **2**. Pathway (2): partial dehydration of sclareol **3** to produce manool **4**, labd-7,14-dien-13-ol **5**, abienol **6** and labd-7,13-dien-15-ol **7**, while further dehydration of these alcohols leads to labd-7,12,14-triene **8** and sclarene **9**

any product under our experimental conditions. In contrary, when TECHNOSA-H2 was applied, a variety of products is obtained (Scheme 3). In Scheme 3, starting from sclareol **3**, the product mixture can involve MO compounds **1** and **2** i.e. cyclic ether, mixture of C13 epimers (pathway 1) or several alcohols i.e. partial dehydration products which are manool **4**, labd-7,14-dien-13-ol **5**, abienol **6** and labd-7,13-dien-15-ol **7** (pathway 2). Further dehydration of the alcohols **4**, **5, 6** and **7** leads to complete dehydration products i.e. labd-7,12,14-triene **8** and sclarene **9**.

3.2 Solvent–Driven Selectivity and Mechanism

Although, yields up to 50% to MO can be obtained in a solvent-free system (Table 1), specific solvents were found to strongly influence the reaction results. For the investigation of solvent applicability in the catalytic conversion of sclareol to MO, several polar and non-polar solvents have been tested at the same reaction conditions (reaction time = 10 min, T = 66 °C), as shown in Table 1. The reaction temperature of 66 °C was chosen, as it constitutes the lowest boiling point temperature of the tested solvents.

In the tests with dimethylformamide, no reaction took place as the solvent blocked the reactivity of the acid sites of the catalyst. Therefore, basic polar solvents are considered as inappropriate solvents for the investigated "zeolite catalyst-solvent" system.

Inspection of Table 1 shows that the higher selectivities in MO were achieved when sclareol is initially dissolved in a glyme-type solvent i.e. diglyme, triglyme, tetraglyme. Glymes, i.e. glycol diethers, are saturated polyethers containing no other functional groups. They are aprotic solvents with high chemical stability [47]. Glymes have a variety of industrial applications and their ability to form hydrogen bonds with the reactants/intermediates of several chemical processes has been extensively studied [47, 49–51].

Taking into account that: (i) sclareol dehydration is highly accelerated over our acid catalyst; (ii) a glyme-type solvent,

Table 1 Manoyl oxide yield from sclareol conversion over TECHNOSA-H2 catalyst combined with various solvents (t = 10 min, T = 66 °C, catalyst weight: 0.9% weight of sclareol) [44–48]

Solvent	Dielectric constant	Boiling point (°C)	Selectivity to MO%
Solvent-free	–	–	50
Dimethylformamide	36.7 (20 °C)	153	No reaction
Tetrahydrofuran	7.6 (20 °C)	66	70
1,4-Dioxane	2.21 (20 °C)	101	76.2
Diglyme (Diethylene glycol dimethyl ether)	7.4 (25 °C)	162	90
Triglyme (Triethylene glycol dimethyl ether)	7.62 (25 °C)	218	89
Tetraglyme (Tetraethylene glycol dimethyl ether)	7.79 (25 °C)	275	88.9
Hexane	1.9 (20 °C)	69	65
Dodecane	2.01 (20 °C)	212	66

which can interact with sclareol via hydrogen bonds formation, increases the MO selectivity, while the non-hydrogen bond forming solvents don't; and (iii) the variety of the partial dehydration products of Scheme 3 obtained over the TECHNOSA-H2 catalyst indicating that water elimination starts either from OH group being in the ring of sclareol or from the other one being in the side chain, we can propose the catalytic mechanism illustrated in Scheme 4.

According to this mechanism when "TECHNOSA-H2–Glyme" system is applied (Scheme 4), formation of hydrogen bonds between the glyme solvent and OH groups of sclareol takes place. The formation of these hydrogen bonds changes the configuration of sclareol in order to minimize the distance between its hydroxyl groups. Then an acidic proton from the catalyst surface attacks to the C_{13} oxygen of sclareol. As follows, the protonated hydroxyl group is substituted by the C_8 oxygen and leads to the production of MO along with the formation of one water molecule. The respective procedure follows when the acidic proton attacks to the C_8 hydroxyl group of sclareol. Based on the reaction results, it is seen that there is not any preference in the attack of the acidic proton of TECHNOSA-H2, but it randomly attacks C_8 or C_{13} oxygen of sclareol. This is proved by the ratio of the C_8 and C_{13} alcohols that are each time produced which differs from test to test.

From the process described in Scheme 4 the final product is a mixture of the C13 isomers of MO. This is in line with previous research [26] where it is shown that the initial C13 configuration of sclareol does not limit the synthesis of 13R- or 13S-MO.

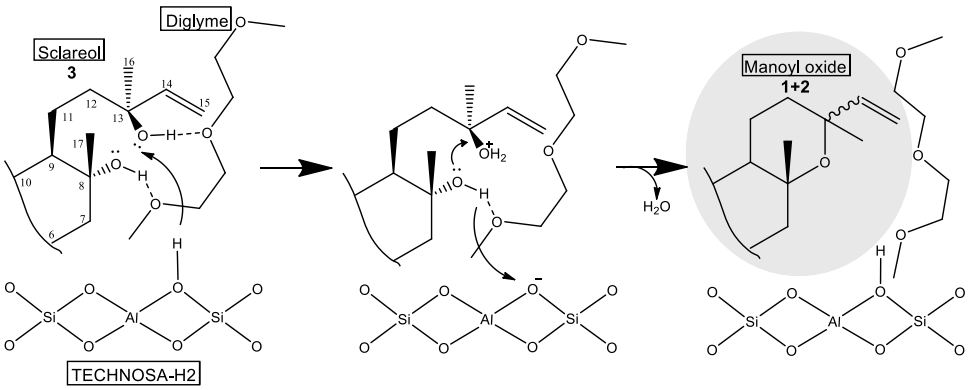

Scheme 4 Proposed mechanism using the "TECHNOSA-H2–Glyme" system for the conversion of sclareol (**3**) to manoyl oxide (**1 + 2**)

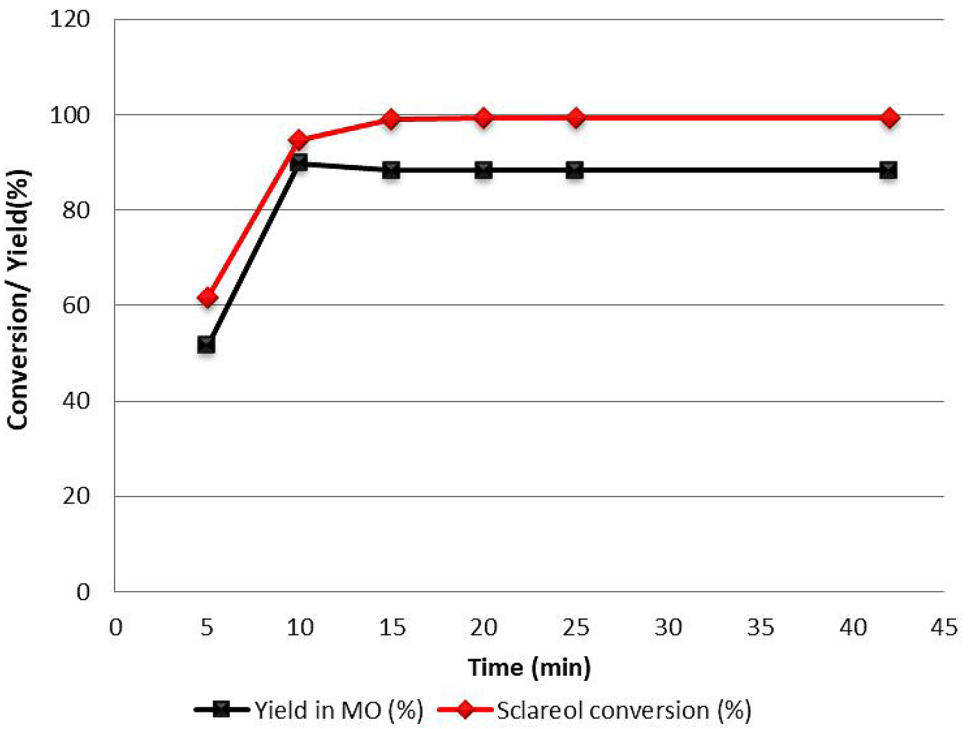

Fig. 1 Conversion of sclareol and yield of manoyl oxide (MO) obtained over TECHNOSA–H2 catalyst, using triglyme as solvent at various reaction times (temperature = 135 °C, catalyst weight = 0.9% weight of sclareol)

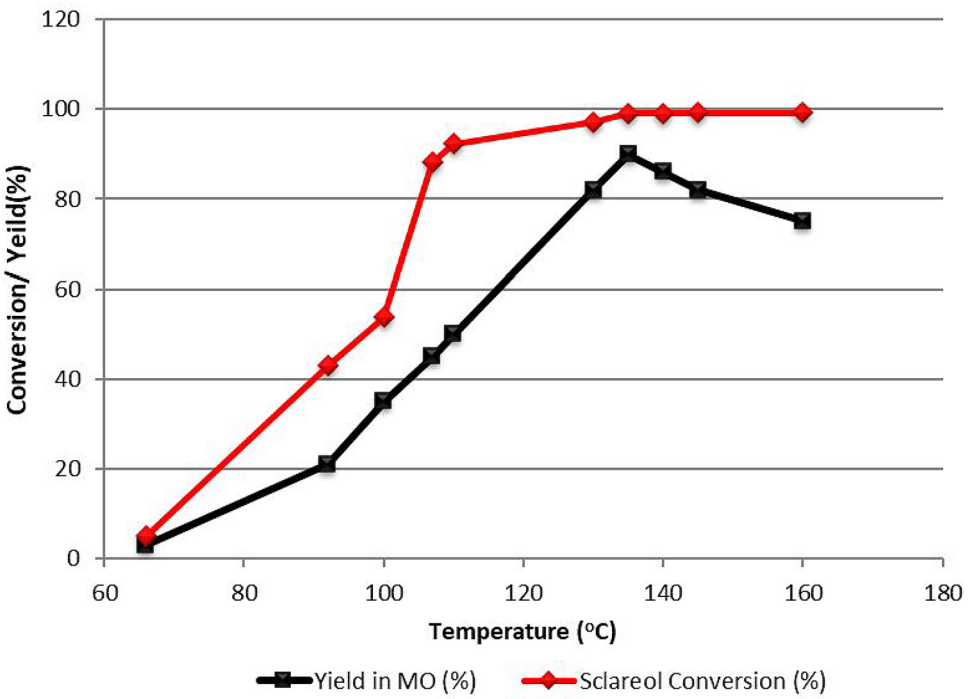

Fig. 2 Conversion of sclareol and yield of manoyl oxide (MO) obtained over TECHNOSA–H2 catalyst, using triglyme as solvent at various temperatures (reaction time = 10 min, catalyst weight = 0.9% weight of sclareol)

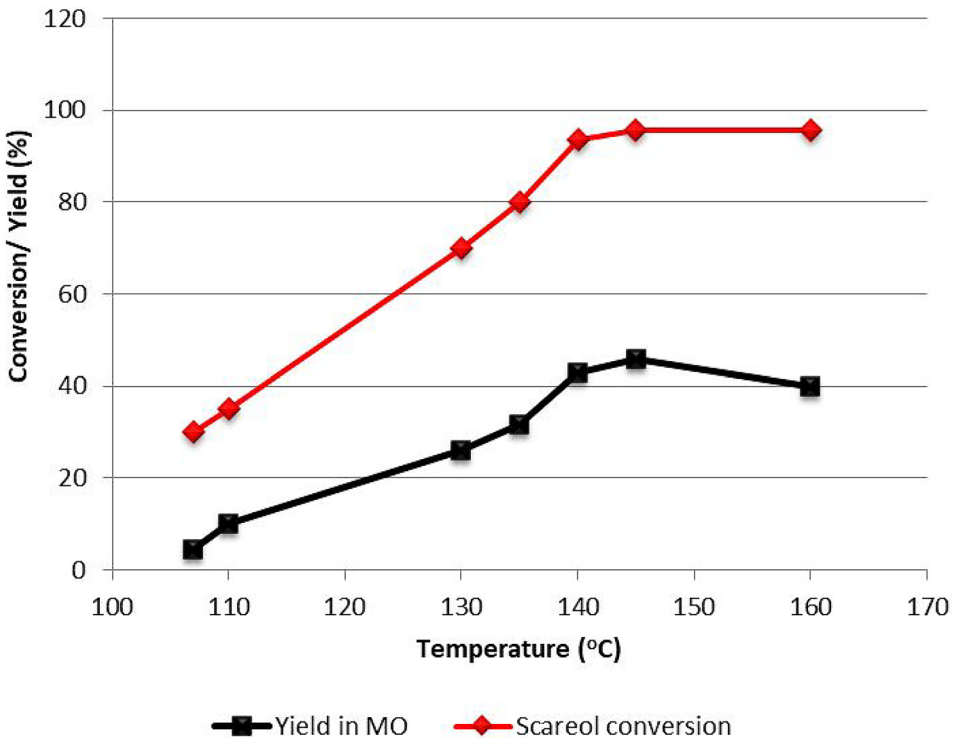

Fig. 3 Conversion of sclareol and yield of manoyl oxide (MO) obtained over TECHNOSA–H2 catalyst, using dodecane as solvent at various temperatures (reaction time = 10 min, catalyst weight = 0.9% weight of sclareol)

3.3 Activation Energy Calculation

Figure 1 illustrates time optimization measurements at 135 °C, where it is shown that at reaction times equal to 10 min the optimum yield for MO is achieved when triglyme is used as solvent. Figures 2 and 3 present the percentage conversion values of sclareol and the yields of MO achieved at various reaction temperatures (up to 160 °C) under the same reaction conditions but combining TECHNOSA–H2 catalyst either with a glyme-type solvent

(Fig. 2) or a non-polar solvent (Fig. 3). Thus, one can make a direct comparison of the effects of the aforementioned types of solvents on the title reaction. The solvents that were chosen for this comparison were triglyme and dodecane, since they both have high boiling point values and they represent polar and non-polar solvents, respectively. The results obtained confirmed the successful cooperation of a glyme-type solvent with the TECHNOSA–H2 catalyst in the whole reaction temperature range studied. Taking into account that the highest MO yield was achieved at ~ 135 °C one can conclude that a glyme-type solvent (like triglyme) with boiling point higher than 135 °C is a good choice for the studied reaction.

Using the results presented in Fig. 2 and Fig. 3 and assuming first order kinetics up to 135 °C for triglyme and up to 145 °C for dodecane, we calculated the reaction constant (k) values at various reaction temperatures using Eq. (1)

$$k = -\frac{\ln(1-x)}{t} \quad (1)$$

where x and t stand for yield in MO and reaction time, respectively. By the insertion of x and t for various reaction temperatures to the above equation, the energetics of the reaction pathway which leads only to MO and not to the total amount of the reaction products, can be calculated (Table S1). Introducing these values in an Arrhenius plot, we obtained a very good linear correlation as shown in Supplementary material (Fig.S1), which confirms the aforementioned first order assumption. Using the slope of the straight line obtained for the tests with triglyme as solvent, we calculated an activation energy value, $E_a = 62.70 \pm 0.1$ kJ mol^{-1}. On the other hand, using the slope of the straight line obtained for the tests with dodecane as solvent the activation energy value was calculated to be $E_a = 93.46 \pm 0.16$ kJ mol^{-1}.

From the above results, we can safely assume that indeed the use of glyme-type solvents changes the energetics of the reaction network for the conversion of sclareol, to favour the formation of the desired product. The activation energy barrier for sclareol dehydration to MO (Scheme 3: reaction pathway 1) is decreased in the presence of the glyme-type solvent (62.70 kJmol^{-1}), whereas the same barrier is higher when dodecane is used as solvent (93.46 kJmol^{-1}). The critical role of glyme-type solvents in the mechanistic pathways and the yield of the reaction to the desired product is therefore confirmed.

Finally, additional experiments have been performed in air-free conditions, using nitrogen as the inert gas. It was shown that such conditions do not alter the product distribution.

Table 2 Textural and acid properties of the catalysts TECHNOSA-H2, TECHNOSA-H2C and TECHNOSA-A2 [42, 43]

Catalyst	Property	
	S_{BET} (m^2/g)	Equilibrium pH
TECHNOSA-H2	236	2.65
TECHNOSA-H2C	242	4.47
TECHNOSA-A2	72	4.21

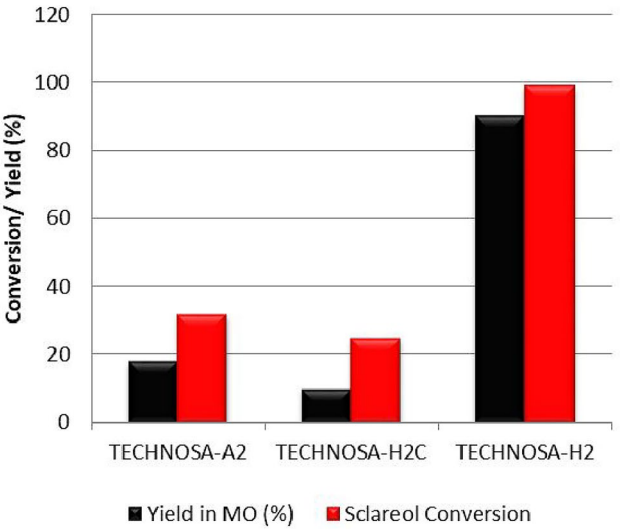

Fig. 4 Conversion of sclareol and yield of manoyl oxide (MO) achieved over TECHNOSA–H2, TECHNOSA-H2C and TECHNOSA-A2 catalyst (solvent triglyme, t = 10 min, T = 135 °C)

3.4 Investigation of the Effect of BET Surface Area and Acidity of the Catalyst

In order to investigate the influence of the surface area and the acidity of the catalyst to the reaction results, two more catalysts were prepared and studied. These are TECHNOSA-H2C (prepared via air-calcination of TECHNOSA-H2 at 500 °C for 2 h) and TECHNOSA-A2 (natural mordenite activated with acetic acid). The properties of the catalysts tested are presented in Table 2.

The value S_{BET} concerns all the pores of the catalyst including micropores (≤ 2 nm), mesopores (2-50 nm) and macropores (larger than 50 nm) and the external surface as well [52]. The equilibrium pH of a dense "solid/water" suspension is an easily determined parameter and indicates the acidity of the solid surface [53]. Sclareol conversion and MO yield over the catalysts TECHNOSA-H2, TECHNOSA-H2C and TECHNOSA-A2 are shown in Fig. 4.

Inspection of Fig. 4 and Table 2 reveals that the acidity of the catalyst is the key factor determining the catalytic performance. Indeed, the highest sclareol conversion and MO yield is obtained over the TECHNOSA-H2 catalyst which has the

highest acidity (lowest equilibrium pH). The aforementioned kinetic parameters are dramatically decreased over the TECHNOSA-H2C catalyst, which has the lowest acidity among the catalysts studied although it exhibits similar S_{BET} value with its non-calcined counterpart (Table 2). On the other hand, the TECHNOSA-A2 catalyst with considerably lower S_{BET} value but somewhat higher acidity than the TECHNOSA-H2C catalyst exhibits slightly higher conversion of sclareol and yield of MO than those obtained over the latter catalyst.

4 Conclusions

According to the results presented the water elimination from sclareol is accelerated over the strong acid catalyst (TECHNOSA-H2) studied in this work. However, in absence of a solvent or in the presence of an inappropriate solvent this elimination is random leading in variety of dehydration products.

The mechanism of the catalytic dehydration reaction of sclareol was investigated and it was shown that sclareol can be dehydrated leading to either the formation of a cyclic ether which is a mixture of MO C13 epimers or the formation of several alcohols. Further dehydration of the produced alcohols leads to the synthesis of totally dehydrated compounds which are labd-7,12,14-triene and sclarene.

To control the product distribution towards the desired compound, a solvent-driven selectivity of the natural mordenite acid catalyst is proposed. The combination of TECHNOSA-H2 catalyst with a glyme type solvent increases the yield of the cyclic ether MO. The key to success for this controllable system is the use of the solvent polarity as an effective strategy to regulate the linkage between sclareol and the acid catalyst and modify the inter-molecular distances.

The effect of the solvent was proved by comparing the product distribution when a glyme-type solvent is used, towards other polar and non-polar solvents. Finally, we can safely assume that indeed the use of glymes as solvents alters the energetics of the reaction network, since the activation energy barrier for sclareol dehydration to afford MO is decreased in the presence of a glyme solvent (62.70 $kJmol^{-1}$), whereas the same barrier is higher using dodecane as solvent (93.46 $kJmol^{-1}$).

Finally, the influence of the BET surface and the acidity of the catalyst was also studied. It has been shown that acidity is a key parameter of catalytic performance in the present reaction.

In contrary with prior art on the synthesis of MO where long reaction times, multistep processes or toxic reagents are involved, our new "TECHNOSA-H2–Glyme" system provides a sustainable alternative to the already mentioned processes. This new system offers high specificity substrate dehydration in a one-step process, where short reaction times (t = 10 min), low temperatures (T = 135 °C) and atmospheric pressure conditions are only involved, resulting to yields in MO of up to 90%.

Our work provides a step forward towards the sustainable synthesis of 13R-MO as a precursor of Ambrox and a promising option for application in the synthesis of Forskolin where the total biosynthetic pathway for Forskolin synthesis can be replaced by a process which combines a chemical catalytic step for the production of 13R-MO, followed by a biosynthetic pathway for the synthesis of Forskolin from 13R-MO.

Supplementary Information The online version contains supplementary material available at https://doi.org/10.1007/s10562-021-03721-6.

Declarations

Conflict of interest Ms. D. Makarouni, Prof. C. Kordulis and Prof. V. Dourtoglou declare that there is no conflict of interest. All co-authors have seen and agree with the contents of the manuscript and there is no financial interest to report.

References

1. Lawson MA, Kaouadji M, Chulia AJ (2008) Nor-dehydrodeguelin and nor-dehydrorotenone, C22 coumaronochromones from Lonchocarpus nicou. Tetrahedron Lett 49(15):2407–2409
2. Tang G-H, Chen Z-W, Lin T-T, Tan M, Gao X-Y, Bao J-M et al (2015) Neolignans from *Aristolochia fordiana* prevent oxidative stress-induced neuronal death through maintaining the Nrf2/HO-1 pathway in HT22 cells. J Nat Prod 78(8):1894–1903
3. Aricò F, Tundo P, Maranzana A, Tonachini G (2012) Synthesis of five-membered cyclic ethers by reaction of 1,4-diols with dimethyl carbonate. Chemsuschem 5(8):1578–1586
4. Hamberger B, Pateraki E, Møllerø BL, Nørholm M, Nielsen MT, Andersen-Ranberg J, et al (2016) Inventors; University of British Columbia Technical University of Denmark Kobenhavns Universitet, assignees. Stereo-specific synthesis of (13r)-manoyl oxide. US Patent 20160318893A1, 13 Nov 2016
5. Kännaste A, Laanisto L, Pazouki L, Copolovici L, Suhorutšenko M, Azeem M et al (2018) Diterpenoid fingerprints in pine foliage across an environmental and chemotypic matrix: Isoabienol content is a key trait differentiating chemotypes. Phytochemistry 147:80–88

6. Nielsen MT, Ranberg JA, Christensen U, Christensen HB, Harrison SJ, Olsen CE et al (2014) Microbial synthesis of the forskolin precursor manoyl oxide in an enantiomerically pure form. Appl Environ Microbiol 80(23):7258–7265
7. Chinou I, Demetzos C, Harvala C, Roussakis C, Verbist J (1994) Cytotoxic and antibacterial labdane-type diterpenes from the aerial parts of *Cistus incanus* subsp. *creticus*. Planta Med 60(01):34–36
8. Hutschenreuther A, Birkemeyer C, Grötzinger K, Straubinger RK, Rauwald HW (2010) Growth inhibiting activity of volatile oil from *Cistus creticus* L. against *Borrelia burgdorferi* s.s. in vitro. Pharmazie 65(4):290–295
9. Demetzos C, Katerinopoulos H, Kouvarakis A, Stratigakis N, Loukis A, Ekonomakis C et al (1997) Composition and antimicrobial activity of the essential oil of *Cistus creticus* subsp. *eriocephalus*. Planta Med 63(5):477–479
10. Pateraki I, Andersen-Ranberg J, Hamberger B, Heskes AM, Martens HJ, Zerbe P et al (2014) Manoyl oxide (13R), the biosynthetic precursor of forskolin, is synthesized in specialized root cork cells in Coleus forskohlii. Plant Physiol 164(3):1222–1236
11. Pateraki I, Andersen-Ranberg J, Jensen NB, Wubshet SG, Heskes AM, Forman V et al (2017) Total biosynthesis of the cyclic AMP booster forskolin from Coleus forskohlii. Elife 6:e23001
12. Cambie RC, Joblin KN, Preston AF (1971) Chemistry of the Podocarpaceae. XXX. Conversion of 8α,13-Epoxylabd-14-ene into a compound with an ambergris-type odour. Aust J Chem 24(3):583–591
13. Yang S, Tian H, Sun B, Liu Y, Hao Y, Lv Y (2016) One-pot synthesis of (−)-Ambrox. Sci Rep 6(1):32650
14. Ncube EN, Steenkamp L, Dubery IA (2020) Ambrafuran (AmbroxTM) synthesis from natural plant product precursors. Molecules 25(17):3851
15. Wagh VD, Patil PN, Surana SJ, Wagh KV (2012) Forskolin: upcoming antiglaucoma molecule. J Postgrad Med 58(3):199
16. Yousif MH, Thulesius O (1999) Forskolin reverses tachyphylaxis to the bronchodilator effects of salbutamol: an in-vitro study on isolated Guinea-pig trachea. J Pharm Pharmacol 51(2):181–186
17. Godard MP, Johnson BA, Richmond SR (2005) Body composition and hormonal adaptations associated with forskolin consumption in overweight and obese men. Obes Res 13(8):1335–1343
18. Dubey MP, Srimal RC, Nityanand S, Dhawan BN (1981) Pharmacological studies on coleonol, a hypotensive diterpene from Coleus forskohlii. J Ethnopharmacol 3(1):1–13
19. Haye B, Louis Aublin J, Champion S, Lambert B, Jacquemin C (1985) Chronic and acute effects of forskolin on isolated thyroid cell metabolism. Mol Cell Endocrinol 43(1):41–50
20. Mora-Pale M, Sanchez-Rodriguez SP, Linhardt RJ, Dordick JS, Koffas MA (2014) Biochemical strategies for enhancing the in vivo production of natural products with pharmaceutical potential. Curr Opin Biotechnol 25:86–94
21. Schalk M, Pastore L, Mirata MA, Khim S, Schouwey M, Deguerry F et al (2012) Toward a biosynthetic route to sclareol and amber odorants. J Am Chem Soc 134(46):18900–18903
22. Ignea C, Ioannou E, Georgantea P, Trikka FA, Athanasakoglou A, Loupassaki S et al (2016) Production of the forskolin precursor 11β-hydroxy-manoyl oxide in yeast using surrogate enzymatic activities. Microb Cell Fact 15(1):46
23. Andersen-Ranberg J, Kongstad KT, Nielsen MT, Jensen NB, Pateraki I, Bach SS et al (2016) Expanding the landscape of diterpene structural diversity through stereochemically controlled combinatorial biosynthesis. Angew Chem Int Ed 55(6):2142–2146
24. Mastan A, Rane D, Dastager SG, Vivek Babu CS (2021) Molecular insights of fungal endophyte co-inoculation with Trichoderma viride for the augmentation of forskolin biosynthesis in Coleus forskohlii. Phytochemistry 184:112654
25. Forman V, Bjerg-Jensen N, Dyekjær JD, Møller BL, Pateraki I (2018) Engineering of CYP76AH15 can improve activity and specificity towards forskolin biosynthesis in yeast. Microb Cell Factories 17(1):181
26. Vlad PF, Russo AG, Lazur'evskii GV (1966) Synthesis of manoyl oxide and 13-epimanoyl oxide. Chem Nat Compd 2(3):139–141
27. Moulines J, Lamidey A-M, Bats J-P, Morisson V (1993) A short and efficient synthesis of (+)-13-epimanoyl oxide from sclareol. Synth Commun 23(21):2991–2998
28. Jensen NB, inventor; Evolva Holding SA (2016) Assignee. Methods and materials for biosynthesis of manoyl oxide. US Patent 10208326B2, 19 May 2016
29. Carey C, inventor; Koste Biochemicals, Koste Biochemicals Sas (2016) Assignes. Process for the Cyclodehydration of Diols and Use Thereof for the Manufacturing of Ambrafuran and Other Cycloether Derivatives. US Patent 9469622B2, 18 Oct 2016
30. Alvarez-Manzaneda EJ, Chaboun R, Alvarez E, Cabrera E, Alvarez-Manzaneda R, Haidour A et al (2006) Cerium(IV) ammonium nitrate (CAN): a very efficient reagent for the synthesis of tertiary ethers. Synlett 2006(12):1829–1834
31. Koval'skaya SS, Kozlov NG, Kulcitki V, Aricu A, Ungur N (2013) Transformation of sclareol under ritter reaction conditions. Russ J Org Chem 49(2):303–311
32. Zhang C, Ju H, Lu C-Z, Zhao F, Liu J, Guo X et al (2019) High-titer production of 13R-manoyl oxide in metabolically engineered *Saccharomyces cerevisiae*. Microb Cell Factories 18(1):73
33. Makarouni DP, Dourtoglou V (2018) Inventors; Vioryl Chemical and Agricultural Industry, Research S.A, assignee. Conversion of sclareol to manoyl oxide under mordenite catalysis. Europian Patent 3409663 A1, 31 May 2018
34. Ihm SK, Chung MJ, Park KY (1988) Activity difference between the internal and external sulfonic groups of macroreticular ion-exchange resin catalysts in isobutylene hydration. Ind Eng Chem Res 27(1):41–45
35. Koujout S, Brown DR (2004) The influence of solvent on the acidity and activity of supported sulfonic acid catalysts. Catal Lett 98(4):195–202
36. Tejero J, Cunill F, Iborra M, Izquierdo JF, Fité C (2002) Dehydration of 1-pentanol to di-n-pentyl ether over ion-exchange resin catalysts. J Mol Catal A 182–183:541–554
37. Cunill F, Tejero J, Fité C, Iborra M, Izquierdo JF (2005) Conversion, selectivity, and kinetics of the dehydration of 1-pentanol to Di-n-pentyl ether catalyzed by a microporous ion-exchange resin. Ind Eng Chem Res 44(2):318–324
38. Mellmer MA, Sener C, Gallo JMR, Luterbacher JS, Alonso DM, Dumesic JA (2014) Solvent effects in acid-catalyzed biomass conversion reactions. Angew Chem Int Ed 53(44):11872–11875
39. Ordomsky VV, van der Schaaf J, Schouten JC, Nijhuis TA (2012) The effect of solvent addition on fructose dehydration to 5-hydroxymethylfurfural in biphasic system over zeolites. J Catal 287:68–75
40. Vanoye L, Zanota M-L, Desgranges A, Favre-Reguillon A, De Bellefon C (2011) Solvent effects in liquid-phase dehydration reaction of ethanol to diethylether catalysed by sulfonic-acid catalyst. Appl Catal A 394(1):276–280
41. Makarouni D, Lycourghiotis S, Kordouli E, Bourikas K, Kordulis C, Dourtoglou V (2018) Transformation of limonene into p-cymene over acid activated natural mordenite utilizing atmospheric oxygen as a green oxidant: a novel mechanism. Appl Catal B 224:740–750
42. Lycourghiotis S, Makarouni D, Kordouli E, Bourikas K, Kordulis C, Dourtoglou V (2018) Activation of natural mordenite by various acids: characterization and evaluation in the transformation of limonene into p-cymene. Mol Catal 450:95–103
43. Lycourghiotis S, Makarouni D, Kordouli E, Bourikas K, Kordulis C, Dourtoglou V (2020) The influence of calcination on the

physicochemical properties of acid activated natural mordenite. Curr Catal 9(2):138–147
44. Smallwood I (2012) Handbook of organic solvent properties. Butterworth-Heinemann, Oxford
45. Maryott AA, Smith ER (1951) Table of dielectric constants of pure liquids. U.S. Government Printing Office, Washington DC
46. Wohlfarth C (2008) Static dielectric constant of tetraethylene glycol dimethyl ether. Static dielectric constants of pure liquids and binary liquid mixtures: supplement to volume IV/17. Springer, Berlin
47. Tang S, Zhao H (2014) Glymes as versatile solvents for chemical reactions and processes: from the laboratory to industry. RSC Adv 4(22):11251–11287
48. Cox ER (1935) Boiling points of normal paraffin series. Ind Eng Chem 27(12):1423–1425
49. Fromm KM, Goesmann H, Bernardinelli G (2000) H-bonded polymer structures of different dimensionality: syntheses and crystal structures of [Ca(DME)n(H2O)m]I2·(DME)x (1: n=3, m=3, x=1; 2: n=2, m=4, x=0) and [Ca{CH3(OCH2)3OCH3}(H2O)4]I2. Polyhedron 19(15):1783–1789
50. Jaycox GD, Sinta R, Smid J (1982) Complexes of polyacids with poly(vinylbenzocrown ether)s and polyvinylbenzoglymes in water. J Polym Sci 20(6):1629–1638
51. Arnáiz FJ, Aguado R, Pedrosa MR, Mahía J, Maestro MA (2001) Outer-sphere addition compounds of MoO2Br 2(H2O)2 with ethers. Molecular structure of MoO2Br2(H2O)2 L (L=2,5,8-trioxanonane; 2,5,8,11,14-pentaoxapentadecane). Polyhedron 20(22):2781–2785
52. Barrett EP, Joyner LG, Halenda PP (1951) The determination of pore volume and area distributions in porous substances. I. Computations from nitrogen isotherms. J Am Chem Soc 73(1):373–380
53. Vakros J, Kordulis C, Lycourghiotis A (2002) Potentiometric mass titrations: a quick scan for determining the point of zero charge. Chem Commun 17:1980–1981

Authors and Affiliations

Dimitra Makarouni[1,2] · Christos Kordulis[1,3,4] · Vassilis Dourtoglou[2,5]

[1] Department of Chemistry, University of Patras, 26504 Patras, Greece

[2] VIORYL, Chemical and Agricultural Industry, Scientific Research S.A, 28th km. Athens-Lamia national road, 19014 Afidnes, Greece

[3] Foundation of Research and Technology-Institute of Chemical Engineering Science (FORTH/ICE-HT), Stadiou Str. Platani, P.O. Box 1414, 26500 Patras, Greece

[4] School of Science and Technology, Hellenic Open University, Tsamadou 13-15, 26222 Patras, Greece

[5] Department of Wine, Vine and Beverage Sciences, University of West Attica, 12243 Athens, Greece